H2020-FETOPEN-2019-01

FET-Open Challenging Current Thinking

POSEIDON

NanoPhOtonic devices applying Self-assembled colloIDs for novel ON-chip light

Starting date of the project: 01/01/2020
Duration: 48 months

= Deliverable D4.3 =

Report on electrically pumped light sources

Due date of deliverable: 31/12/2023
Actual submission date: 07/02/2024

WP and Lead Beneficiary: WP4, UHull
Version: V1.0

Dissemination level		
PU	Public	x
CO	Confidential, only for members of the consortium (including the Commission Services)	
CI	Classified, information as referred to in Commission Decision 2001/844/EC	

This project has received funding from the European Union's Horizon 2020 research and innovation programme under grant agreement No 861950.

AUTHOR

Author	Organization	Contact (e-mail, phone)
Ali Adawi	UHULL	a.adawi@hull.ac.uk
Jean-Sebastien Bouillard	UHULL	j.bouillard@hull.ac.uk
Alina Muravitskaya	UHULL	a.muravitskaya@hull.ac.uk
Jeremy Baumberg	UCAM	jjb12@cam.ac.uk
Shu Hu	UCAM	sh2065@cam.ac.uk

DOCUMENT DATA

Keywords	plasmonic, nano-antenna, electrical pumping, nano-light sources
Point of Contact	Name: Ali Adawi Partner: UHull Address: Department of Physics and Mathematics Robert Blackburn Building University of Hull Cottingham Road Hull, Hu6 7RX UK Phone:+44-1482-465037 E-mail:a.adawi@hull.ac.uk

DISTRIBUTION LIST

Date	Issue	Recipients
07/02/2024	V1.0	EC & all partners through OwnCloud

REVIEW PROCESS

Document version	Date	Status/Change
V0.1	19/12/2023	Draft
V0.2	18/01/2024	Final Draft
V1.0	07/02/2024	Final

VALIDATION PROCESS

Reviewers		Validation date
Work Package Leader	Ali Adawi (UHULL)	18/01/2024
Project Coordinator	Stephan Suckow	07/02/2024

Executive Summary

In this deliverable, the methods used to develop electrically pumped plasmonic nano-light sources and electrically controlled plasmonic nano-scattering sources are reported. These developments are crucial for achieving photonic integrated circuits and tunable plasmonic sensors. Various plasmonic antenna geometries are explored, among them, nanoparticle on mirror (NPoM) antenna, which has been verified as one of the best systems for creating electrically pumped light source. By successfully integrating an ultrathin electron blocking layer of PEDOT:PSS into the plasmonic nano-light sources, a 1000-fold increase in the device lifetime was achieved compared to devices without the electron blocking layer. The recorded electroluminescence (EL) spectra from the developed devices showed a clear splitting in the EL signal demonstrating for the first-time strong coupling from a single plasmonic cavity under ambient conditions. The Stark effect was used to electrically control the scattering response of NPoM antennas. Under applied electric field, the scattering spectra follow the quadratic Stark shift. The developed approach provides a promising and reliable way for achieving electrically tuned plasmonic devices for real-time sensing applications and to interrogate the excitonic properties of semiconductor materials at the nanoscale.

The report includes:

- the integration of a monolayer of QDs into NPoM antennas and
- the creation of ultracompact electrically pumped plasmonic nano-light sources (~100 nm size).
- The integration of an electron blocking layer of PEDOT:PSS into the NPoM-QD antenna devices.
- The optoelectronic characterisation of the electrically pumped NPoM-QD nano-light sources.
- The integration of a 20 nm polymer layer into NPoM antennas
- and the creation of electrically controlled scattering sources.
- The scattering characterisation of the fabricated antennas under electrical bias.

Table of contents

Introduction

Creating an integrable, electrically pumped light source is paramount for the development of photonic integrated circuits[1]. Semiconductor quantum dots (QDs) emerge as promising candidates to achieve this goal due to their high quantum yield, stability, and tunable band gap[2]. However, a grand challenge remains to create an electrically pumped device of ultracompact size, long term stability and high emission rate. Plasmonic nanocavities, which confine light to extremely small sub-wavelength volumes, offer an exceptional solution to this challenge[3].

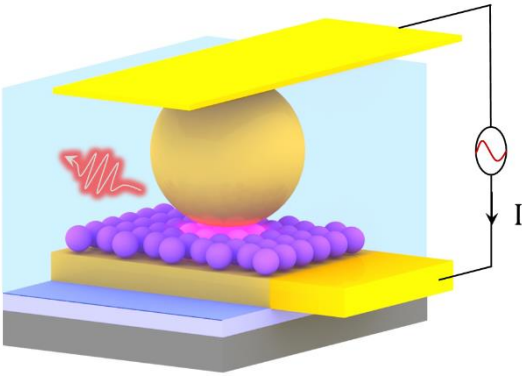

***Figure 1**. Schematics of electrically pumped nanoparticle on mirror antennas.*

Here, we report on integrating QDs into plasmonic nanocavities and create an ultracompact electrically pumped device (~100 nm size). We explore various plasmonic antenna geometries (as discussed in deliverable D4.2), with the nanoparticle on mirror (NPoM) antenna verified as one of the best configurations so far for creating such an electrically pumped light source. We successfully integrate a highly uniform monolayer of QDs into such NPoM nanocavities using liquid-air self-assembly, which shows extremely high consistency of photoluminescence signatures and also high yield of strong coupling devices. We develop new strategies to create electrical contacting of these NPoM-QD antennas, where we obtain electrically pumped light emission of 10^5 counts/s, even without hole- or electron-blocking layers. More importantly, we explore possibilities to integrate ~3 nm or even atomically-thin (graphene) electron (or hole) blocking layers into the ultracompact plasmonic nanocavity-QD devices. This successfully extends the device lifetime by a further 1000-fold, underscoring its potential for practical applications.

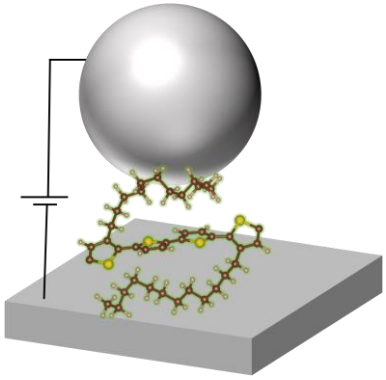

***Figure 2**. Schematic of the electrically tuned plasmonic nanogap.*

In the second part of this report, we discuss the development of electrically driven and actively tunable plasmonic nanogaps. This is an essential requirement for a wide range of applications such as sensing and nanophotonic devices. The transition energies of a material can be modified via the application of an external electric field, also known as the Stark effect[4]. This alters the dielectric function of the nanogap region providing a reliable approach to electrically tune the optical response of a plasmonic nanogap. We successfully utilised the Stark effect to control the scattering response of a plasmonic nanogap formed between a silver nanoparticle and an extended silver film (NPoM) separated by a 20 nm gap of organic semiconductor (see Figure 2). Under an applied electric field, we found that the scattering spectra follow a quadratic Stark shift with a maximum observed red shift of 26 nm. In addition, our approach allowed us to experimentally determine the polarizability of semiconductor material embedded in a nanogap region with spatial resolution below the diffraction limit, offering a new approach to probe the excitonic properties of extremely thin semiconducting materials.

Results and discussion

1. Electrically pumped plasmonic nano-light sources

1.1 Device fabrication

A strategy that combines colloidal self-assembly and lithography is developed for fabricating electrically pumped NPoM antenna devices. Firstly, 50 nm Au is evaporated through a patterned mask to create the bottom Au stripes (Fig. 3). A close-packed monolayer of QDs and Au nanoparticles (NPs) are then transferred on top using liquid-air assembly (see deliverable D4.1). An insulting layer of PMMA (~100 nm) is spin-coated on top followed by O_2 plasma etching to expose the top part of the Au NPs. The top contacting of 12 nm thick Au stripes is created by Au evaporation through the mask with 90° rotation. The final device is a crossbar junction which only allows charge transport to take place through NPoM junctions with QDs as spacers.

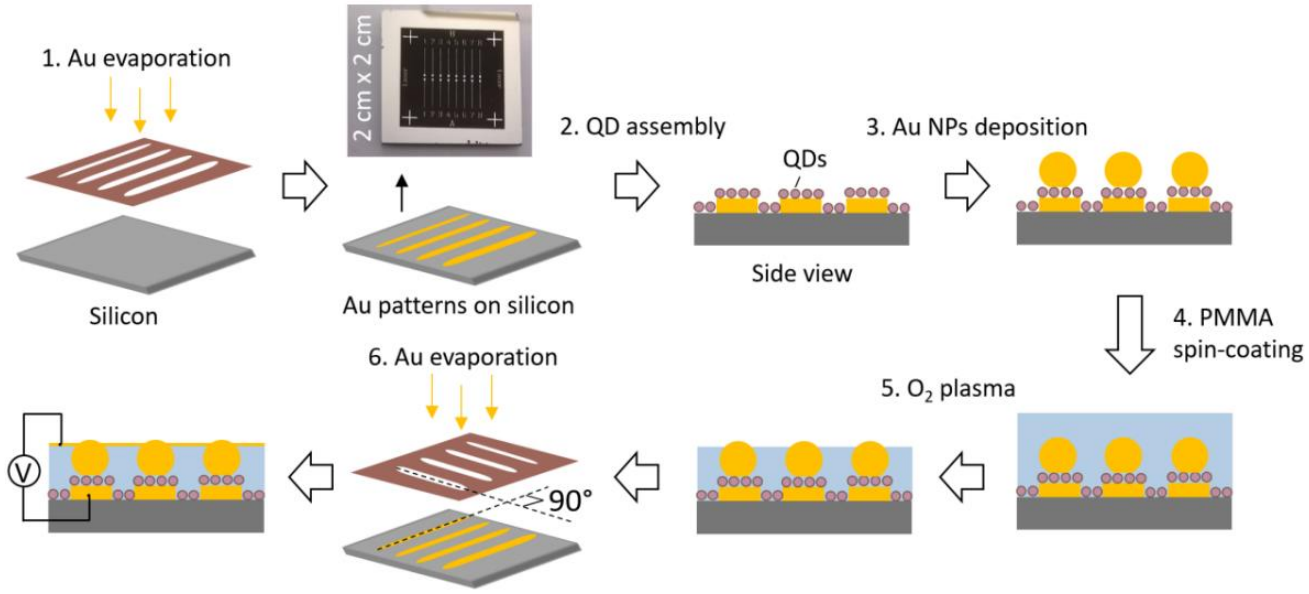

***Figure 3**. Schematic fabrication route for electroluminescent NPoM LED devices*

1.2 Device characterization

To evaluate the performance of this route to antenna fabrication, we performed various characterizations of the NPoM-QD system such as dark field microscopy, transmission electron microscopy (TEM) and photoluminescence (PL) spectroscopy. The monolayer CdSe/ZnS QD films exhibit high uniformity under dark field microscopy (Fig. 4b,c) and transmission electron microscopy (TEM, Fig. 4d), which is already scalable to the centimetre scale (inset in Fig. 4c). More importantly, the PL of such QD monolayers shows extremely small energy variation of ~4 meV (Fig. 4g) over large areas and is stable in time at ambient conditions. NPoM antennas are seen as of identical red color (Fig. 4b), indicating their energy is highly consistent and well matched with the energy transition of the QDs. As a result, one observes strong coupling split-peak characteristics with high yields (74%) in our system (Fig. 4e,f) based on statistical characterization of 840 NPoMs. This is due to mixing between plasmon (NPoM) and exciton (QD) states in the strong coupling regime that forms upper ($\omega+$) and lower ($\omega-$) polariton states (Fig. 4e) separated by Rabi splitting energy Ω. These results strongly demonstrate the efficient and consistent coupling between QDs and NPoM nanocavities, which is crucial for further development of electrically pumped devices.

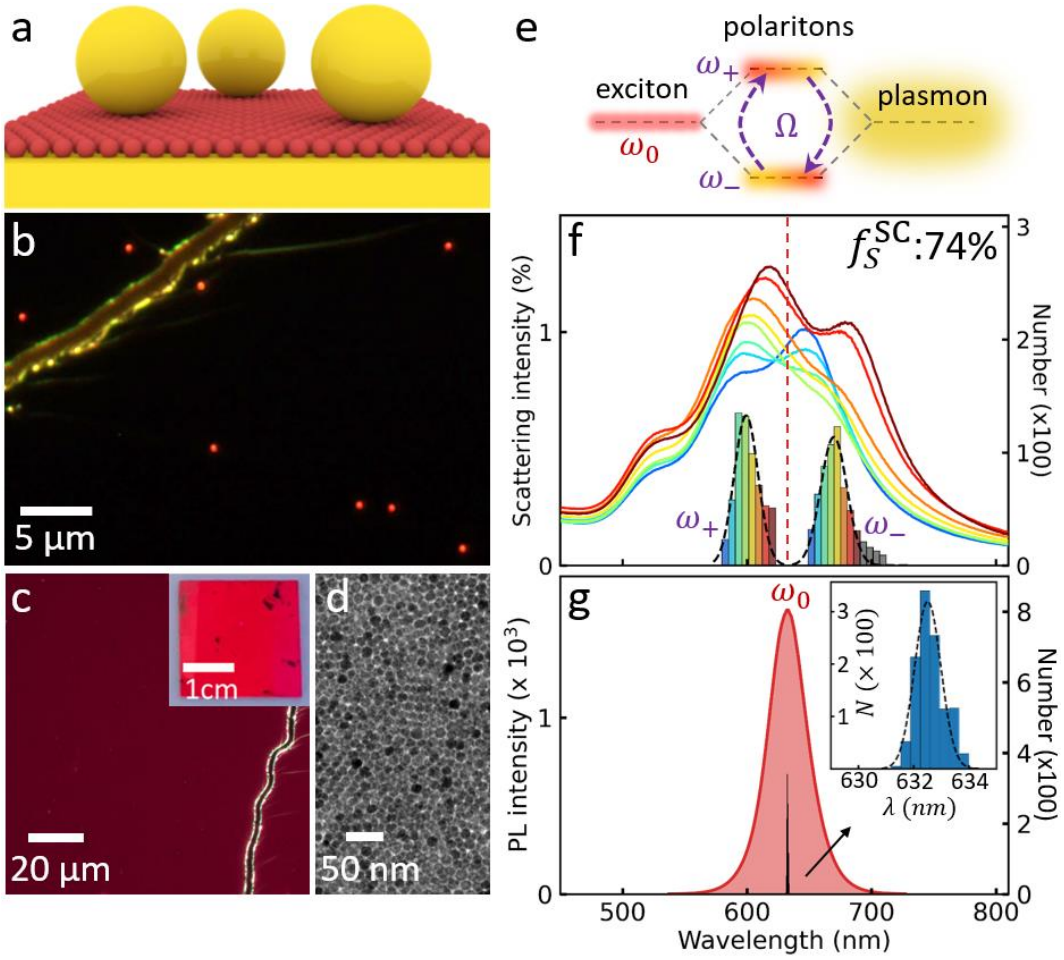

Figure 4. ***a***, *Schematic and* ***b***, *dark-field image of monolayer QDs integrated into nanoparticle-on-mirror (NPoM) nanocavities.* ***c***, *Dark-field and* ***d***, *TEM images of QD monolayer on* (***c***) *Si and* (***d***) *TEM grid. Red color in* (***c***) *is photoluminescence of QDs under illumination. The inset in* (***c***) *shows the assembly on a 2x2 cm² substrate.* ***e***, *Exciton (QD) and plasmon (cavity) hybridization forms polaritons in strong coupling regime.* ***f***, *Average scattering spectra of >800 NPoMs sorted into bins which all show clear energy splitting of coupled modes. Histogram (black dashed) and average spectra are sorted according to energy of lower (ω−) and upper (ω+) polaritons.* ***g***, *Typical photoluminescence spectrum (red) of monolayer QD film in (c), with spectral distribution of exciton peak at different locations (expanded in inset).*

We create electrically pumped devices based on the optimized geometry shown in Fig. 5a. The electrically pumped emission is obtained by gradually applying a DC bias of up to 2 V, that matches the first exciton energy of the QDs (Fig. 5b), originating from a diffraction limited spot and giving integrated count rates of $>10^5$ cts/s (Fig. 5b). The current intensity exhibits a rapid surge upon initiation of the EL due to charge stabilization processes within the ligand layer or ligand rearrangements. Afterwards, the current returns to an average of 0.5 µA, indicating the attainment of an equilibrium situation. Although fluctuations of both current and EL intensity are observed, no distinct correlation can be extracted from them. This may due to the fact that EL depends on local field fluctuations throughout the QD from moving defects and charges, while current fluctuations primarily are controlled by instabilities in the contact barriers near the interfaces. The emission profile of the devices is characterized by k-space spectroscopy (Fig. 5c), where both PL and EL emit in a broad angular range spanning from 0° to 55°. A sustained emission over >3 mins is obtained even for such a simple design, demonstrating the robust performance of such devices under DC bias pumping. The splitting of the EL spectrum (Fig. 5d) indicates the system is still within the strong coupling regime after the device fabrication.

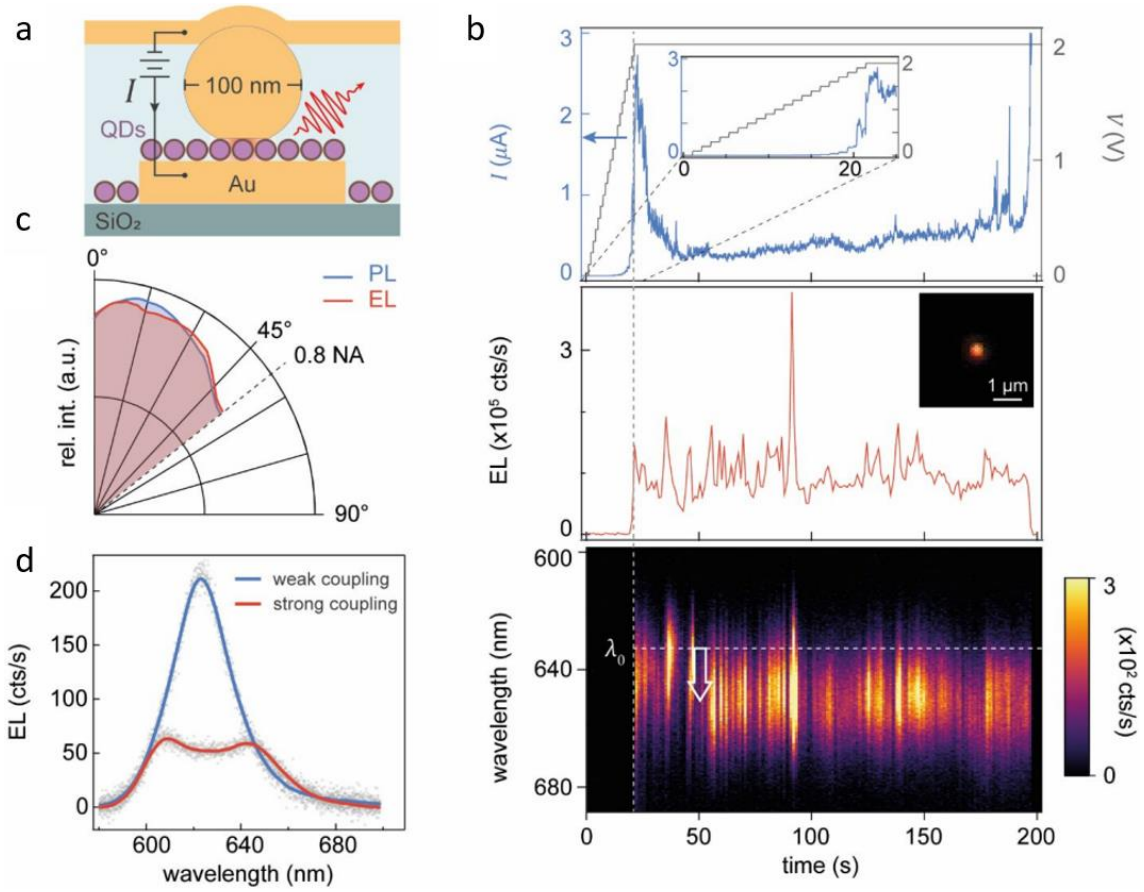

Figure 5. ***a***, *Schematic of single junction electroluminescence (EL) experiment.* ***b***, *Top panel: bias voltage (grey) and current (blue) vs time during electrical pumping of a single QD NPoM device; middle panel: time trace of total EL intensity and EL image (inset); bottom panel: time evolution of QD EL spectrum. Maximum EL count rates exceed 400kcts/s.* ***c***, *Experimental angular emission pattern using optical (blue) and electrical (red) excitation, with 0° normal to the sample plane.* ***d***, *EL spectra of nanoantenna-dressed QD in weak (blue) and strong (red) coupling regimes.*

1.3 Device optimization

To further extend the lifetime of these devices, we explore routes to integrate electron or hole blocking layers into the NPoM-QD antenna devices. Suitable layer integration is required to be only a few nanometers thick since the ultra-small inter-metallic gap is crucial for maintaining large field enhancements in the nanocavity, which remains a grand challenge. To introduce an electron blocking layer at the top electrode, we synthesize a core-shell nanoparticle (Fig. 6a) using wet-chemical processes, adding a PEDOT:PSS layer which can be controlled to the few nanometer range (Fig. 6b). Statistics on >300 NPoMs show the layer remains highly uniform (Fig. 6c), while characterization by Raman spectroscopy (Fig. 6d) demonstrates the presence of the PEDOT:PSS layer.

The effect of this electron blocking layer is verified by using synthesized core-shell Au NPs in device fabrication (Fig. 7a,b). This intervention increases the device lifetime by a factor of 1000 (Fig. 7c), which underscores its potential for practical application. A significant improvement in stability could also be demonstrated by obtaining light emission at a large bias of 12 V (Fig. 7d), revealing large Stark shifts.

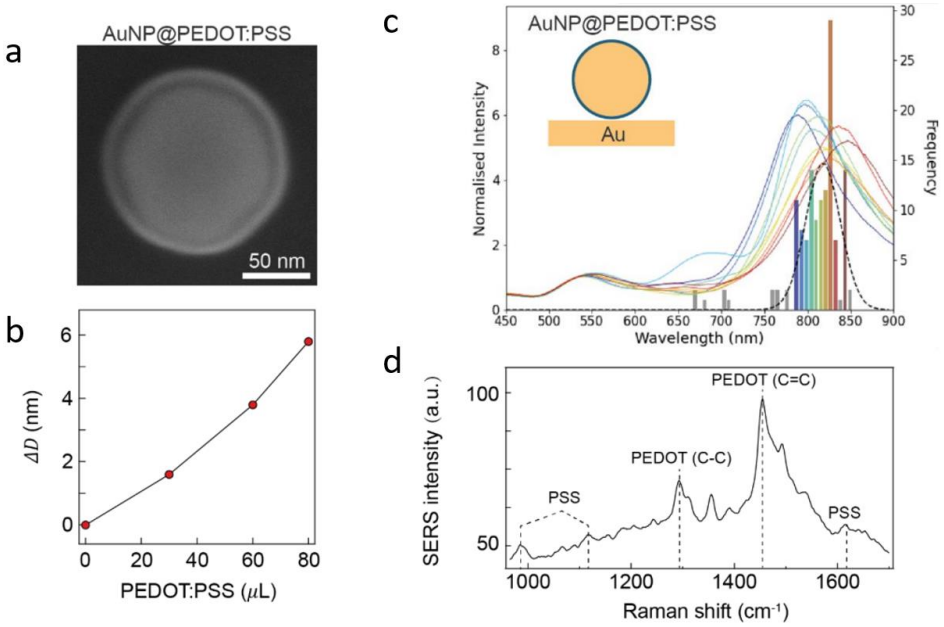

***Figure 6**. **a**, SEM image shows the core-shell structure of the PEDOT:PSS coated AuNP. **b**, Increased polymer coating thickness characterised using dynamic light scattering, as a function of PEDOT:PSS solution volume used in the incubation process. The highest shell thickness (with 80 μL) was used in measurements (**c**). **c**, Distribution of PEDOT:PSS core/shell NPoM (inset) dark-field scattering coupled-mode resonances. Averages of spectra in each histogram bin of the corresponding colours exhibit a centre wavelength of 815 nm. **d**, Surface-enhanced Raman spectrum of PEDOT:PSS core/shell NPoM (λ_{ext} = 633 nm), showing characteristic vibration signatures of PEDOT and PSS.*

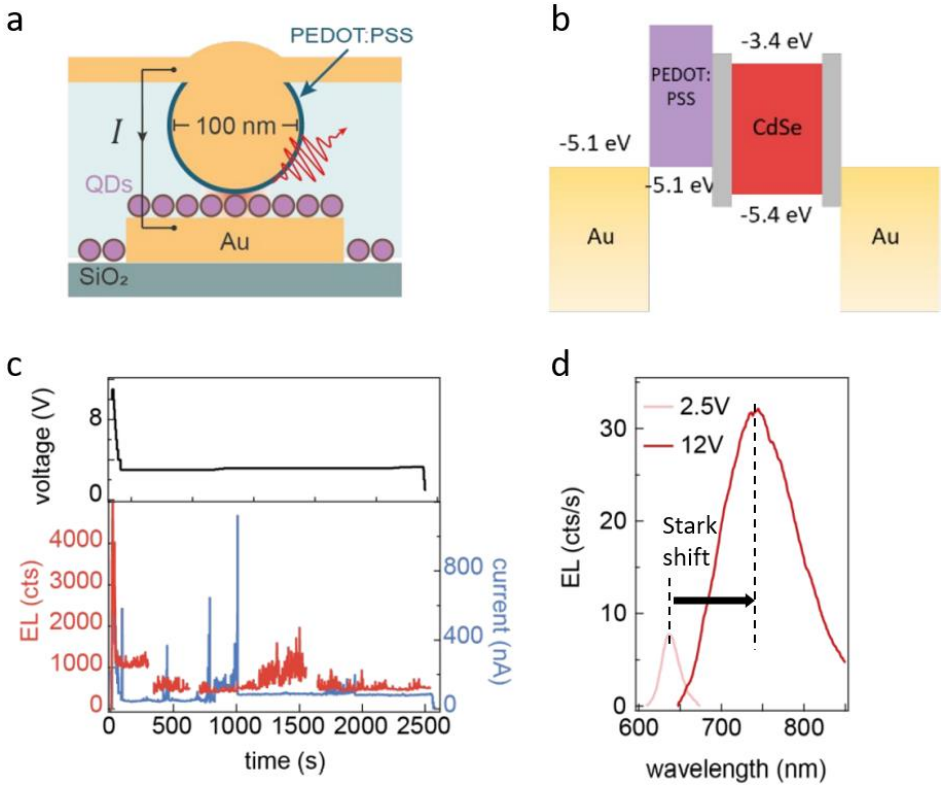

***Figure 7**. **a**, Schematic illustration for single junction electroluminescence (EL) experiment with PEDOT:PSS coated NPoM, where polymer on top of AuNP was etched away, enabling direct contact to the top electrode. **b**, Flat-band energy level diagram of the NPoM device junction. Time traces of (**c**) bias voltage, (**d**) current (blue), and EL intensity during electrical pumping of a single PEDOT:PSS-QD NPoM device. The EL intensity was measured using a Lumenera Infinity miscroscope camera. Breaks in the time trace are due to software data processing. (**e**) EL spectra acquired at 2.5 V and 12 V.*

The above study strongly demonstrates the dramatic effect of integrating an electron blocking layer even just on one side of the electrical junction. Consequently, the device could be further optimized by integrating blocking layers on both sides. However, the inter-metallic gap will then be significantly larger, which decreases the field enhancement of the nanocavity. To address this issue, we worked on integrating graphene (with atomic thickness) into the device (Fig. 8a). As a preliminary exploration, we used two different routes (Fig. 8b,c) for graphene integration. Although the graphene is successfully integrated into the NPoM-QD antenna, our laser marking route is currently limited by the roughness of the substrate while a direct transfer route increases the number of shorted junctions. Further work will be focusing on patterning the graphene along with the substrate, using photolithography.

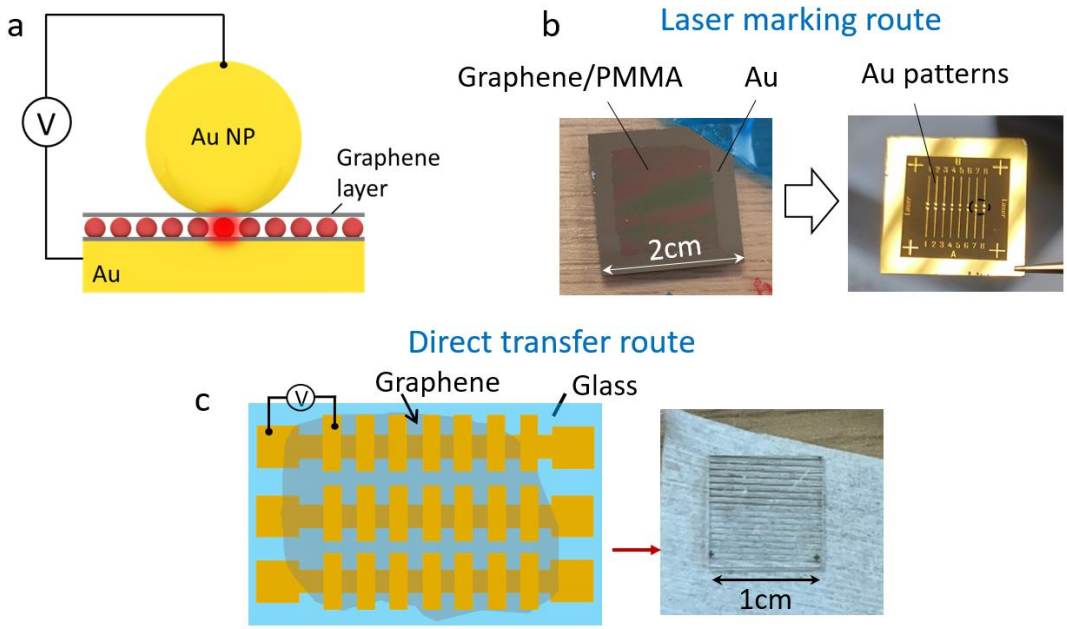

Figure 8. ***a***, *Schematic of the designed electrically pumped device with graphene as the insulting layers.* ***b***, *Laser marking route to pattern the graphene along with Au substrate.* ***c***, *Direct transfer route to integrate the graphene into the antenna device.*

2. Electrically controlled plasmonic nano-scattering sources

To fabricate an electrically driven plasmonic nanodevice we used the following strategy[4]. First, we coated a glass substrate with a 100 nm silver layer forming the device bottom electrode, on top of which 20 nm of the conjugated polymer PQT-12 (Poly[bis(3-dodecyl-2-thienyl)-2,2'-dithiophene-5,5'-diyl]) (see Figure 9a and Figure 9b) was deposited by spin-coating a $10\ g \cdot L^{-1}$ solution of PQT-12 in toluene at a speed of 1500 rpm for 50 s. To complete the plasmonic nanogap, spherical silver nanoparticles of 100 nm diameter suspended in an aqueous solution at a concentration of $2 \times 10^{-2}\ g \cdot L^{-1}$ were spin-coated onto the conjugated polymer surface. Top electrical contact was achieved by thermally evaporating 15 nm of silver on top of the plasmonic nanogap as schematically illustrated in Figure 9b. Figure 9c shows an optical image of the fabricated electrically driven nanogap devices, alongside a typical dark-field image of the devices surface, Figure 9d. To characterise the scattering properties of the fabricated devices, the nanogap was illuminated by white light at an angle of 45^{o} using a long working distance 10x Mitutoyo objective of numerical aperture $NA = 0.28$, and the scattered light was collected at normal incidence using a 50× Mitutoyo objective lens with NA = 0.55. Figure 10a shows two typical scattering spectra on and off the nanogap. On the nanogap, the spectrum exhibits two plasmon modes labelled as M1 and M2, while the spectrum off the nanogap is featureless, indicating that the measured scattered signal stems from the nanogap. Here, the plasmonic modes spectrally overlap with the absorption spectrum and emission spectrum[5] of PQT-12, opening the possibility to modify these processes using our nanogaps. Also, this overlap allows for the plasmonic response of the device to be tuned with an applied electric field via changes in the absorption of the organic semiconductor using the Stark effect.

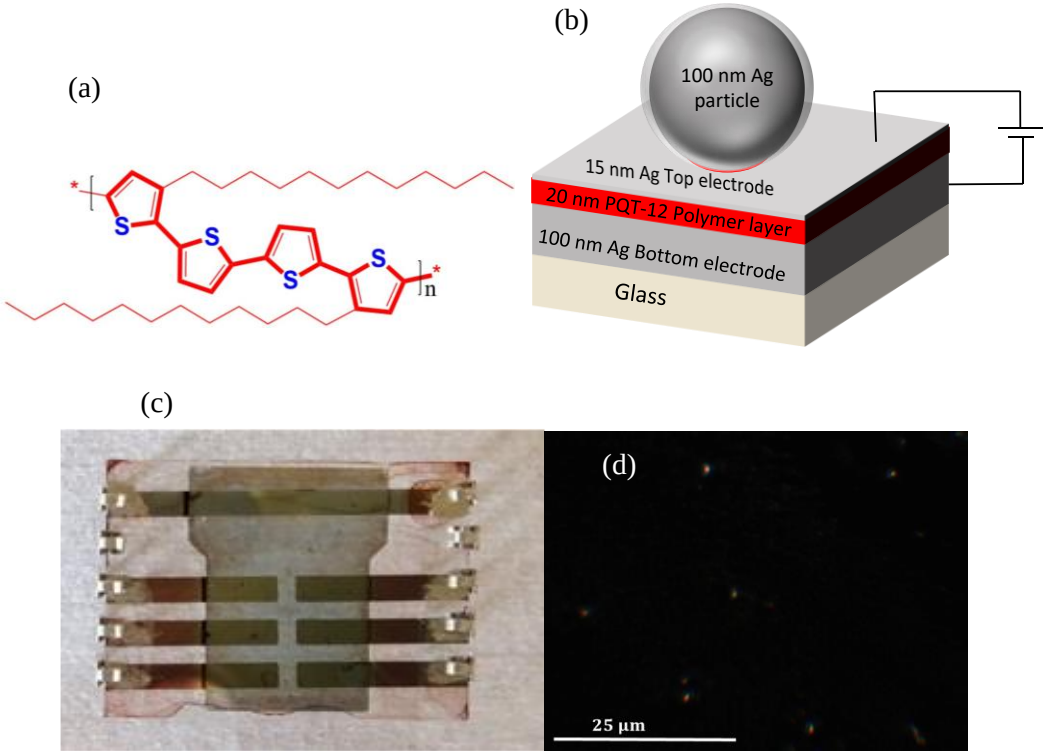

***Figure 9**. (a) Chemical structure of the polymer PQT-12. (b) Schematic illustration of the developed electrically tuned plasmonic nanogap. (c) Picture of the fabricated devices. (d) Dark-field image of the fabricated nanogap.*

Finite difference time domain (FDTD) calculations[4] revealed that mode M1 corresponds to a horizontal dipolar mode, and mode M2 to a vertical dipolar mode (see Figure 10b). The resulting modes in such structures are often described as cavity modes due to specific field distributions in the gap area, with mode M1 having the field distribution of a (1,1) mode and mode M2 the field distribution of (1,0) mode.

Under electrical bias, no emission was detected from our structures, however it was possible to use the applied electric field to tune the scattering properties of the plasmonic nanogap. Figure 11a shows the measured scattering spectra of the nanogap junction as a function of the applied electric field. With increasing the applied electric field, both modes M1 and M2 are redshifted, with a maximum shift of 26 nm for mode M1 and 15 nm for mode M2. The observed

tunability can be linked to the high sensitivity of the nanogap plasmon resonances to small changes in the optical properties of the gap region. In our case, the nanogap region is formed from the organic semiconductor PQT-12, a conjugated polymer characterized by a large oscillator strength and large polarizability, making it sensitive to externally applied electric fields via the Stark effect. The resulting modification of the transition energies of the conjugated polymer PQT-12 under applied electric field alters the material absorption of light. These modifications in the absorption properties of the nanogap region are directly coupled to changes in refractive index via the Kramers-Kronig relation.

In a conjugated polymer, the main dominant term for the Stark effect is the quadratic Stark shift[6] $E(F) = E_0 - \frac{1}{2}\alpha F^2$. Here F is the electric field, E_0 is energy in the absence of electric field, and α is the polarizability of the conjugated polymer.

By fitting our experimental peak position to the quadratic Stark shift equation ($E(F) = E_0 - \frac{1}{2}\alpha F^2$), it is clear our data closely follows the quadratic Stark shift (see Figure 11b). Furthermore, fitting the experimental data to the quadratic Stark shift equation allows to determine the polarizability of the polymer α, yielding $\alpha_1 = 3.7 \times 10^{-23}$ cm^3 for M1, and $\alpha_2 = 1.7 \times 10^{-23}$ cm^3 for M2, with the averaged polarizability value for the whole system $\langle\alpha\rangle = 2.7 \times 10^{-23}$cm^3.

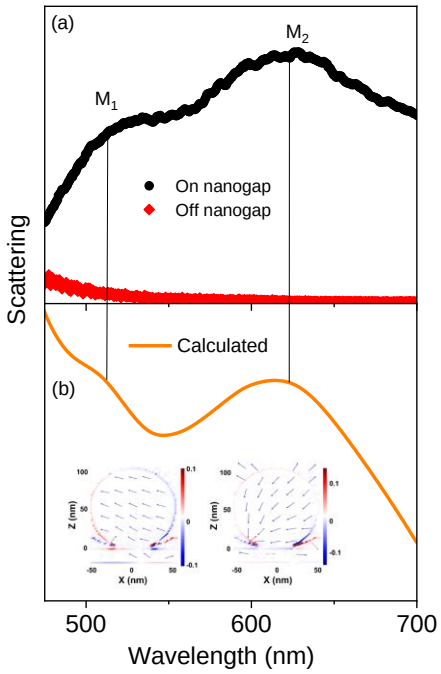

***Figure 10**. (a) Measured scattering spectra taken from the nanogap and away from the nanogap. (b) Calculated scattering spectrum from the nanogap. Insert shows the charge distributions of modes M1 and M2.*

We also performed a density functional perturbation theory (DFPT) response calculation[4] to determine the polarizability cartesian tensor of the PQT-12 polymer. The values obtained are shown in table 1. Because spin-coated polymers align their molecular chains parallel to the substrate and the applied electric field in our experiment is perpendicular to the substrate (see figure 11d), we are probing the polarizability perpendicular to the polymer propagation axis, namely along the αα and ββ components of the polarizability tensor in table 1. Consequently, we average the αα and ββ components of the tensor, leading to a value of 75.81×10^{-23} cm^3 for the polarizability perpendicular to the polymer propagation axis, which is in line with the measured value of PQT-12 polarizability.

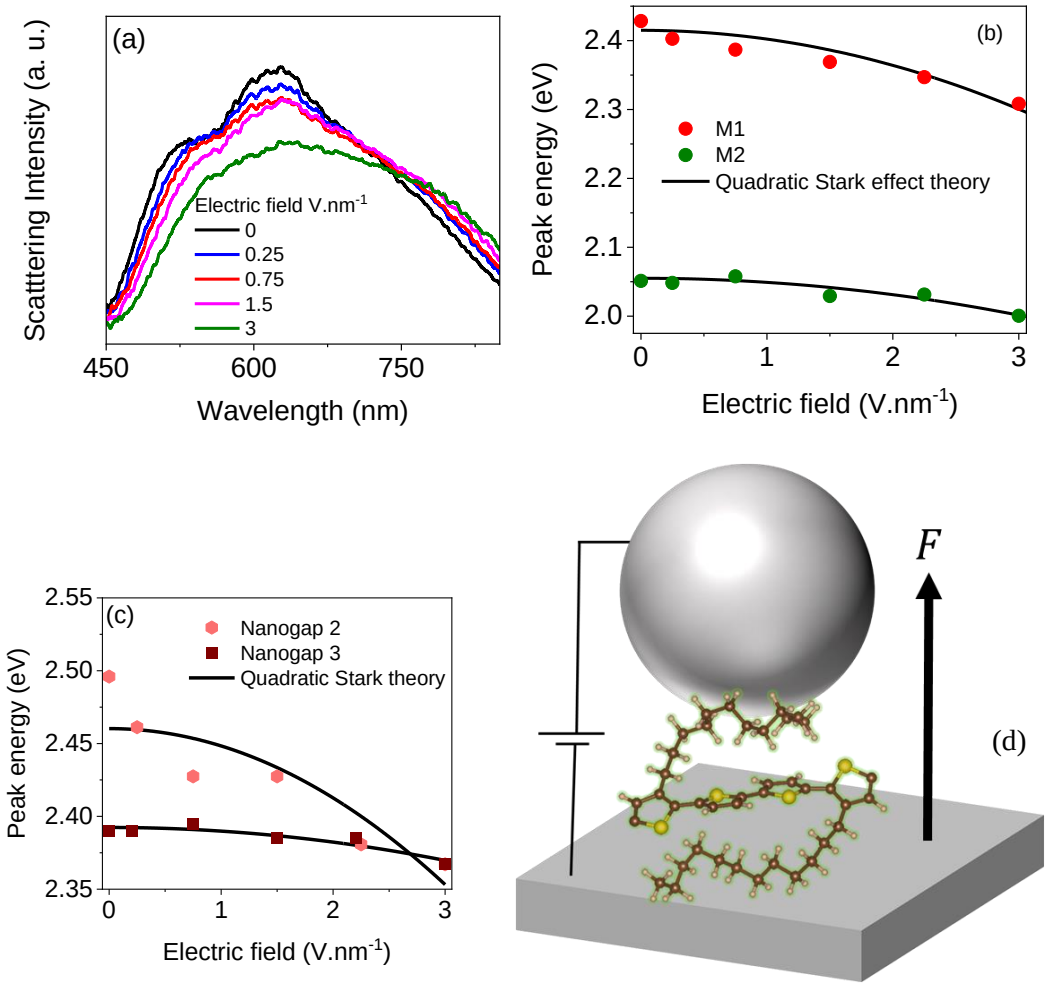

Figure 11. *(a) Measured scattering spectra as a function of applied electric field. (b) Quadratic Stark effect analysis of mode M1 and mode M2. (c) Quadratic Sark effect analysis of two additional nanogaps. (d) Illustration of the applied electric field relative to the polymer chain in the plasmonic nanogap.*

Table 1: *Polarizability tensor of PQT-12 in* 10^{-23} cm^3.

αα	αβ	αγ	ββ	βγ	γγ	⟨αα + ββ⟩	⟨α⟩
5.30	−0.28	0.11	6.31	−0.06	10.73	5.81	2.5

Additionally, the integration of the Stark effect with a plasmonic nanogap offers a powerful method to probe the excitonic properties of semiconducting materials with spatial resolution below the diffraction limit. To demonstrate this potential, we measured the scattering properties of two additional nanogaps. The scattering peak energies of these nanogaps are plotted in figure 11c as a function of the applied electric field. Two different values for the polymer polarizability of 0.7×10^{-23} cm^3 and 3.4×10^{-23} cm^3 were extracted. These differences in the polarizability are attributed to the inhomogeneity and molecular conformation of the polymer on the local level.

In summary, in this section we have demonstrated that the Stark effect can be used to electrically control the scattering response of a plasmonic nanogap formed between a silver nanoparticle and an extended silver film with the gap. Under applied electric field, the scattering spectra follow a quadratic Stark shift with a maximum observed red shift of 26 nm. Furthermore, our approach allows for the experimental determination of the polarizability of semiconductor materials embedded in a nanogap region. The method developed in this work not only provides a promising way for achieving electrically tuned plasmonic devices but also presents a new approach to interrogate the excitonic properties of semiconductor materials at the nanoscale.

Conclusions

- Assembling monolayer QDs on various substrates and antennas is now well established.
- First electrically pumped emission (strong coupling) from a single plasmonic cavity at ambient is achieved.
- Successfully integrating an ultrathin electron blocking layer for creating a highly stable optoelectronic device now gives a 1000-fold increase in lifetime.
- The Stark effect can be utilized to actively control the scattering response of a plasmonic nanogap.
- Scattering spectra follow a quadratic Stark shift with a maximum observed red shift of 26 nm.
- A new approach is developed to interrogate the excitonic properties of semiconductor materials with nanoscale spatial resolution.

3. Degree of progress

The deliverable is 100% fulfilled.

4. Dissemination level

Deliverable 4.3 is public.

5. References

1. E. Pelucchi , G. Fagas , I. Aharonovich , D. Englund, E. Figueroa , Q. Gong, *et al.* The potential and global outlook of integrated photonics for quantum technologies. *Nat. Rev. Phys.* 4, 194-208 (2022).
2. X. Dai ,Z. Zhang, Y. Jin, Y. Niu, H. Cao, X. Liang , *et al.* Solution-processed, high-performance light-emitting diodes based on quantum dots. *Nature* 515, 96-99 (2014).
3. Chikkaraddy R, De Nijs B, Benz F, Barrow SJ, Scherman OA, Rosta E, *et al.* Single-molecule strong coupling at room temperature in plasmonic nanocavities. *Nature* 535, 127-130 (2016).
4. D. Pagnotto, A. Muravitskaya, D. M Benoit, J-S. G. Bouillard, A. M. Adawi, Stark effect control of the scattering properties of plasmonic nanogaps containing an organic semiconductor, *ACS Appl. Opt. Mater.* 1, 1, 500–506 (2023).
5. R. K. Pandey, S. K. Yadav, C. Upadhyay, R. Prakasha, H. Mishra, Surface plasmon coupled metal enhanced spectral and charge transport properties of poly(3,3’’’-dialkylquarterthiophene) Langmuir Schaefer films, *Nanoscale* 7, 6083-6092 (2015).
6. F. Schindler, J.M. Lupton, J. Müller, J. Feldmann, U. Scherf, How single conjugated polymer molecules respond to electric fields. *Nat. Mater. 5* (2), 141– 146 (2006).